

Optical trapping of colloidal particles and cells by focused evanescent fields using conical lenses

Young-Zoon Yoon^{1,2} and Pietro Cicuta^{1*}

¹*Cavendish Laboratory, University of Cambridge, Cambridge CB3 0HE, UK*

²*Department of Physics, Sungkyunkwan University, Suwon 440-746, Korea*

*pc245@cam.ac.uk

Abstract: We demonstrate advantages in terms of trapping force distribution and laser efficiency that come from using a telescopic pair of conical lenses ('axicon') to generate a ring-like beam, that in conjunction with a high NA objective is used for direct optical trapping with a focused evanescent field near a surface. Various field geometries are considered and compared. First, a Gaussian beam and a laser beam focused on the back focal plane of the objective are compared with each other, and they are scanned across the inlet aperture of the objective. This allows to detect the point of total internal reflection, and to study the trapping power near the surface. We confirm that the hollow beam generated by the conical lenses can generate an evanescent field after a high NA objective lens, and that micron-sized particles can be trapped stably. Finally, we apply the focused evanescent field to erythrocytes under flow, showing that cells are trapped against the flow and are held horizontally against the surface. This is a different equilibrium condition compared to conventional single beam traps, and it is particularly favorable for monitoring the cell membrane. We foresee the integration of this type of trapping with the imaging techniques based on total internal reflection fluorescence (TIRF).

© 2010 Optical Society of America

OCIS codes: (140.7010) Laser trapping; (260.6970) Total internal reflection; (170.0170) Medical optics and biotechnology.

References and links

1. A. Ashkin, "Acceleration and trapping of particles by radiation pressure," *Phys. Rev. Lett.* **24**, 156–159 (1970).
2. D. Grier, "A revolution in optical manipulation," *Nature* **424**, 810–816 (2003).
3. J. Meiners and S. Quake, "Femtonewton force spectroscopy of single extended dna molecules," *Phys. Rev. Lett.* **84**, 5014–5017 (2000).
4. Y. Z. Yoon, J. Kotar, G. Yoon, and P. Cicuta, "Non-linear mechanical response of the red blood cell," *Phys. Biol.* **5**, 036007 (2008).
5. D. Axelrod, "Total internal reflection fluorescence microscopy in cell biology," *Traffic* **2**, 764–774 (2001).
6. G. Seisenberger, M. Ried, T. Endreb, H. Buning, M. Hallek, and C. Brauchle, "Real-time single-molecule imaging of the infection pathway of an adeno-associated virus," *Science* **294**, 1929 (2001).
7. N. Chronis and L. Lee, "Total internal reflection-based biochip utilizing a polymer-filled cavity with a micromirror sidewall," *Lab Chip* **4**, 125–130 (2004).
8. J. Wang, N. Bao, L. Paris, R. Geahlen, and C. Lu, "Total internal reflection fluorescence flow cytometry," *Anal. Chem.* **80**, 9840–9844 (2008).
9. S. Kawata and T. Sugiura, "Movement of micrometer-sized particles in the evanescent field of a laser beam," *Opt. Lett.* **17**, 772–774 (1992).

10. S. Chang, J. H. Jo, and S. S. Lee, "Theoretical calculations of optical force exerted on a dielectric sphere in the evanescent field generated with a totally-reflected focused gaussian beam," *Opt. Commun.* **108**, 133–143 (1994).
11. E. Almaas and I. Brevik, "Radiation forces on a micrometer-sized sphere in an evanescent field," *J. Opt. Soc. Am. B* **12**, 2429–2438 (1995).
12. M. Lester and M. Nieto-Vesperinas, "Optical forces on microparticles in an evanescent laser field," *Opt. Lett.* **24**, 936–938 (1999).
13. S. Kuriakose, X. Gan, J. W. M. Chon, and M. Gu, "Optical lifting force under focused evanescent wave illumination: A ray optics model," *J. Appl. Phys.* **97**, 083103 (2005).
14. V. Ruiz-Cortes and J. Vite-Frias, "Lensless optical manipulation with an evanescent field," *Opt. Express* **16**, 6600–6608 (2008).
15. D. Ganic, X. Gan, and M. Gu, "Trapping force and optical lifting under focused evanescent wave illumination," *Opt. Express* **12**, 5533–5538 (2004).
16. Y. Zhang and J. Bai, "Simple and high efficient optical trapping using a cylindrical lens and a single plane wave of incidence," *Opt. Commun.* **281**, 4824–4828 (2008).
17. M. Righini, A. S. Zelenina, C. Girard, and R. Quidant, "Parallel and selective trapping in a patterned plasmonic landscape," *Nat. Phys.* **3**, 477–480 (2007).
18. L. Huang, S. J. Maerkl, and O. Martin, "Integration of plasmonic trapping in a microfluidic environment," *Opt. Express* **17**, 6018–6024 (2009).
19. M. Righini, C. Girard, and R. Quidant, "Light-induced manipulation with surface plasmons," *J. Opt. A: Pure Appl. Opt.* **10**, 093001 (2008).
20. P. Chaumet, A. Rahmani, and M. Nieto-Vesperinas, "Optical trapping and manipulation of nano-objects with an apertureless probe," *Phys. Rev. Lett.* **88**, 123601 (2002).
21. K. Okamoto and S. Kawata, "Radiation force exerted on subwavelength particles near a nanoaperture," *Phys. Rev. Lett.* **83**, 4534–4537 (1999).
22. M.L. Juan, R. Gordon, Y. Pang, F. Eftekhari and R. Quidant, "Self-induced back-action optical trapping of dielectric nanoparticles," *Nat. Phys.* **5**, 915–919 (2009).
23. C. Mellor and C. Bain, "Array formation in evanescent waves," *ChemPhysChem* **7**, 329–332 (2006).
24. M. Gu, J. Haumonte, Y. Mischeau, J. W. M. Chon, and X. Gan, "Laser trapping and manipulation under focused evanescent wave illumination," *Appl. Phys. Lett.* **84**, 4236 (2004).
25. B. Jia, X. Gan, and M. Gu, "Direct observation of a pure focused evanescent field of a high numerical aperture objective lens by scanning near-field optical microscopy," *App. Phy. Lett.* **86**, 131110 (2005).
26. M. Gu, S. Kuriakose, and X. Gan, "A single beam near-field laser trap for optical stretching, folding and rotation of erythrocytes," *Opt. Express* **15**, 1369–1375 (2007).
27. I. Manek, Y. Ovchinnikov, and R. Grimm, "Generation of a hollow laser beam for atom trapping using an axicon," *Opt. Commun.* **147**, 67–70 (1998).
28. V. Garces-Chavez, D. McGloin, H. Melville, W. Sibbett, and K. Dholakia, "Simultaneous micromanipulation in multiple planes using a self-reconstructing light beam," *Nature* **419**, 145–147 (2002).
29. D. Ivanov, V. Shcheslavskiy, I. Markl, M. Leutenegger, and T. Lasser, "High volume confinement in two-photon total-internal-reflection fluorescence correlation spectroscopy," *Appl. Phys. Lett.* **94**, 083902 (2009).

1. Introduction

Optical trapping is based on the fact that a light beam propagating through interfaces between dielectric objects is able to transfer momentum and generate forces on the objects. Typically a high intensity and high gradient are required to obtain a confining force, and a strongly focussed laser beam is used as a source of light [1]. Tweezers are used to manipulate and to measure forces, in the range between 0.01 and 100pN. The standard type of optical tweezers has found widespread use to address a variety of biological questions in recent years [2–4]. In many experiments, the beam is used to manipulate a colloidal particle, which is used as a "handle" for actuating biological objects (whole cells, membrane protrusions) or molecules (DNA strands, elements of the cytoskeleton). However it is not always possible to design an investigation to include the colloidal probe particle. If the focused light beam is used to trap biological cells directly, there can be various potential problems, ranging from the strong localized heating of the object near the focal point, to the fact that the force itself is applied to a small region, with linear dimension of the order of less than a micron. This makes it difficult to directly trap large thin objects, such as for example the membrane of a eucaryotic cell, which has linear dimension between 10 and 50 micron depending on the cell type. Cell membranes are a region

of strong biological activity, and there is a need to develop techniques for both imaging and manipulation. The idea of using total internal reflection to provide a localized excitation field for fluorescence imaging has proven very successful, and the method is known as TIRF imaging [5–8]. It would be clearly beneficial to have a micromanipulation device capable of maintaining (holding, moving, releasing, etc) the cell membrane within the narrow region near the reflection boundary, where the TIRF excitation is effective, enabling greater control over single molecule detection on cell membranes. We intend this study as a necessary precursor to such promising extensions.

Under total internal reflection (TIR), an evanescent field is generated that has been shown to trap micro- and nano-sized objects [9]. The trapping forces that act on spherical particles in an evanescent field have been studied at various levels of sophistication [10–13]. Of course trapping forces on more complex objects such as biological cells are much more difficult to estimate, and hence the usefulness of approaching this problem experimentally. The condition for TIR can be achieved by either a prism element or a high NA objective. In developing this type of trap with imaging in mind, it is convenient to use high numerical aperture (NA) objective approach [14, 15]. Evanescent field trapping can overcome various problems typical of direct trapping using single beam focused traps. The exponential decay of light intensity induces an optical gradient field towards the boundary interface, which provides a force towards the surface. With infrared light (1064nm wavelength beams are very often used in optical trapping) the field is confined essentially to less than a micron from the surface, and in the case of a suspended cell (roughly spherical in shape) this means that most of the cell interior is not illuminated. The transfer of energy into the object is significantly lower compared to focusing propagating beams on the object surface. Depending on the optical design, the trapping area in the evanescent wave can be made wider than in conventional focused optical trapping.

Several geometries for achieving trapping in evanescent wave illumination have been reported. One possibility is to use the radiation force induced by an evanescent wave produced at the interface between two media under the TIR condition, obtained with cylindrical prism [9, 16]. In this case the strength of the evanescent wave is too weak to trap and manipulate objects. To overcome this weakness it was possible to introduce a metallic tip or pattern to enhance the evanescent field through a surface plasmon effect [17–19]. In the presence of a tip it was shown that a particle of a few nanometers in size in water or air could be trapped [20]. The use of the evanescent field localized near a subwavelength aperture has also been proposed [21] and recently shown experimentally as a route to trap a subwavelength particles [22]. Single beams incident at an angle to the surface generate an evanescent field that carries momentum in the plane of the surface, in the direction of propagation [9]. A simple way to compensate for this force, and obtain a force perpendicular to the surface, is by having a compensating beam from the opposite direction [23]. Another elegant geometry in which the momentum parallel to the surface cancels out relies on obtaining the focused evanescent field from a high NA objective that is centrally obstructed, resulting in a focused ring beam [24–26]. The opaque disk blocks the central disk section of the inlet beam, so that after the objective the convergence of all rays is larger than the critical angle determined by the interface between two media. However because a part of the beam is blocked, energy is lost, and a high power laser is required to trap particles. In ref [15] the trapping efficiency of this configuration is investigated in detail. An alternative way to generate hollow beams is through the use of a lens and axicon pair, again in combination with a beam stop [27]. The axicon element (a conical lens) is well known to transform a Gaussian beam into a Bessel beam, and in this guise has already found application in optical trapping [28]. We use here the property that a telescopic pair of axicon elements transforms a Gaussian beam into a propagating hollow beam. Using this geometry, the hollow annular beam can be generated without loss, and by directing this beam into a high NA objective a focused

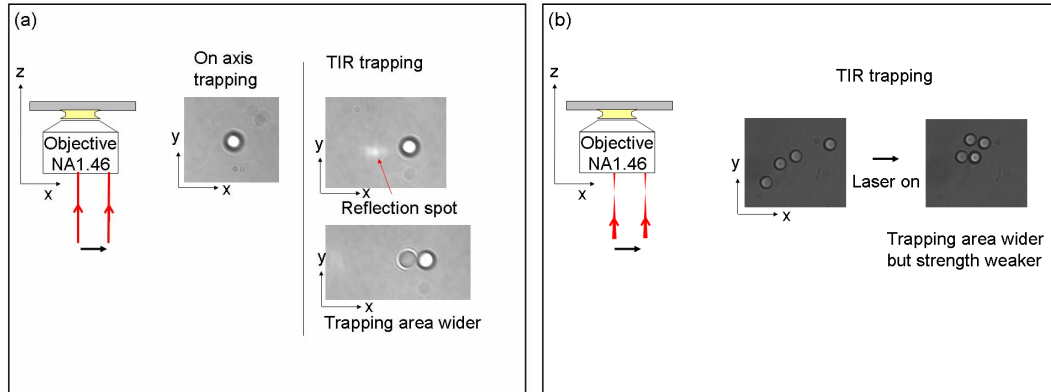


Fig. 1. Silica beads of $3\mu\text{m}$ diameter can be trapped on the bottom of the chamber by various beam geometries: (a) Gaussian beam on-axis and off-axis such that with TIR an evanescent field is generated; (b) Weakly focused beam on the back focal plane, leading to an extended trapping region.

evanescent field is obtained. In this study, we demonstrate the direct optical trapping from a focused evanescent field generated by a ring beam using a telescopic pair axicon elements and a high NA objective (NA=1.46). To compare the results obtained with the evanescent field to the conventional trapping with Gaussian beams, we have performed test experiments using a) a narrow Gaussian beam and b) a beam weakly focused on the back focal plane of the objective. In both cases, the beam position is scanned across the inlet of the objective and we investigate the trapping power. We show that red blood cells (erythrocytes) can be trapped near the surface even against a flow force, and that the focused evanescent field leads to a particular equilibrium position for trapped erythrocyte cells, different from what is achieved in conventional trapping.

2. Experiment

The trapping laser beam is generated from a continuous-wave HeNe laser (Melles Griot, 633nm, $P_{max} = 30\text{mW}$). The objective is a high NA lens (Zeiss, Plan-apochromat, oil immersion, NA= 1.46, 100x) with inlet diameter=5mm. The objective is mounted inverted, i.e. the beam is incident from below, and we label z the vertical propagation axis. To investigate trapping by evanescent fields, we use three different setup geometries, having (a) a single Gaussian beam, (b) a focussed beam, and (c) a hollow beam on the back focal plane of the microscope objective. In (a) the laser beam waist is 0.96mm. The distance of the beam from the optical axis at the inlet was varied, as shown in Fig. 1(a). In case (b) three lenses, acting as beam expander ($\times 2.5$) and focusing lens ($f=200\text{mm}$) are added into the setup described above. The beam is focused on the back focal plane, as shown in Fig. 1(b). In case (c) a hollow beam is generated in order to make a focused evanescent field: Two conical lenses (Axicon, Del Mar Photonics, 160°) are aligned on-axis after the beam expander, as shown in Fig. 2. After the objective lens, immersion oil ($n_{oil}=1.52$) fills the gap to a glass slide of $n_g=1.52$. The glass confines a layer of water ($n_w=1.33$), with a final glass slide providing the top surface. The evanescent wave is set up at the interface between the first glass slide and water. In order to measure the onset of TIR, measurements are taken of the intensity of the vertically propagating beam beyond the sample chamber described here.

To optimize the hollow beam setup, we used the commercial optical simulation software tool ZEMAX. Given the NA of this objective, and the basic relation $NA = n \sin(\theta_{max})$, $\theta_{max} = 74.1^\circ$ is the half-angle of the maximum cone of light that can exit the lens. The critical angle of

incidence for TIR at the glass water interface is $\theta_{crit} = \arcsin(n_w/n_g) = 61.2^\circ$. Considering beams parallel to the optical axis, the beam with incidence angle θ_{max} is the one entering the objective back aperture at the largest possible distance from the center, i.e. 2.5mm. The critical angle corresponds to a beam entering at distance of 1.3mm. Using ZEMAX the positions of the axicon elements have been determined in order to achieve a hollow beam with internal diameter 1.5mm and external diameter close to the aperture edge. Therefore in ideal conditions we expect all of this hollow beam to be reflected back from the glass/water interface. Experimentally we always observe some leakage of light which may be caused by scattering at various optical surfaces.

For imaging, the sample is illuminated from above with a condensed LED ($\lambda = 470\text{nm}$) and is observed in bright field with a CMOS camera (Stingray, Allied Vision Technologies), recording to a PC using customized software (Labview). Video is recorded at ~ 160 frames/s and with pixel size 65nm. To observe the trapping phenomena, silica beads of 3.0, 1.85, 1.0 and 0.5 μm diameter and polystyrene beads of 2.0 μm diameter (Bangs Labs) are used. The beads are tracked automatically from the video data, using a custom image analysis code based on an image correlation matching algorithm (coded in Matlab). The trapping potential is locally described by a harmonic spring, and the trap stiffness is calibrated by measuring the thermal displacements of a trapped bead:

$$P(x) = \frac{1}{\sigma\sqrt{2\pi}} \exp\left(-\frac{(x-x_0)^2}{2\sigma^2}\right), \quad k = \frac{1}{\sigma^2} k_B T, \quad (1)$$

where x is one component of the instantaneous position, x_0 the mean position, $P(x)$ the distribution of position, k_B the Boltzmann constant, T temperature and k the trapping stiffness.

As a first study with a biological sample, fresh red blood cells (RBC) are used. About 100 μl of blood was obtained by a fingertip needle prick from a healthy volunteer donor, and it was diluted into phosphate-buffered saline (PBS) containing acid citrate dextrose at pH 7.4. The RBCs were washed three times by centrifugation and resuspension in the same buffer and finally suspended at about 0.1% haematocrit in PBS containing 1mg/ml bovine serum albumin (BSA) (Sigma-Aldrich). This solution is flowed through a 1mm square glass channel with optical glass sides, under gravity flow (near the surface, free cells are observed to drift with velocity v between 0.6 and 4.6 $\mu\text{m/s}$). In this flow we aim to trap RBCs and show that they can be maintained near the bottom surface, and released back into the flow.

3. Results

The different optical geometries result in varying beam size at the glass/water interface. The trapping area in case (a) of the standard Gaussian beam and case (b) of a beam focussed at the back focal plane are shown in Fig. 1. In case (a), upon scanning across the aperture, the condition of TIR is reached. Here the trapping region is wider than when the beam is on axis. This is shown by the fact that two 3.0 μm diameter beads can be trapped side by side in the direction of the beam deviation off axis. In case (b) as expected the trapping region is much wider and the trapping stiffness is weaker than case (a). The intensity that is transmitted beyond the sample chamber is significantly reduced when the incidence angle on the glass/water interface increases beyond the critical angle; this is shown in Fig. 3(a). Figure 3(b) shows the trapping stiffness for 3 μm diameter silica beads in this case. In the Gaussian beam geometry the trapping stiffness in the x axis direction is lower than the y axis direction (the laser inlet position is scanned along x). At incidence angles where the trapping is through the evanescent field it is observed that the stiffness is one order of magnitude lower than for the propagating field on axis. The trapping stiffness in the focused beam geometry [case (b)] is much weaker (three orders of magnitude) than the Gaussian beam on axis, but the trends as a function of the

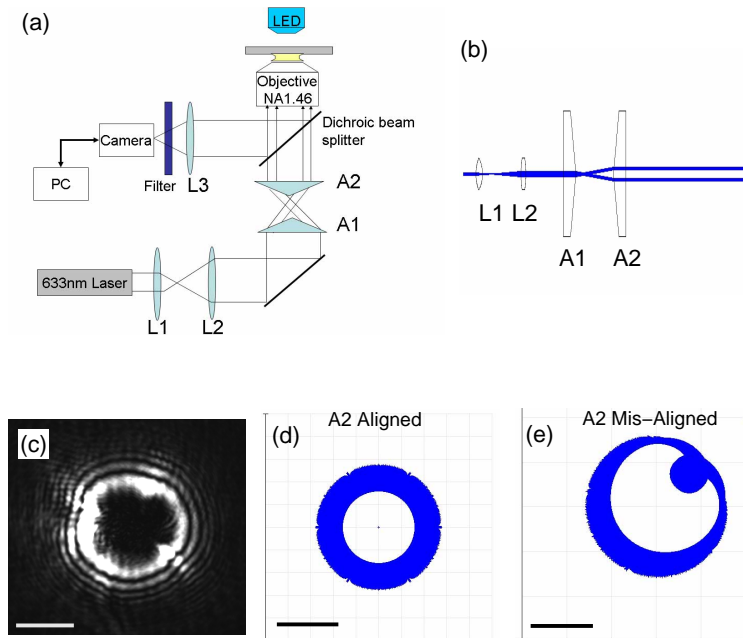


Fig. 2. (a) Schematic diagram of the evanescent-field trapping system using a pair of conical lenses (axicons); (b) Beam intensity from optical simulation of propagation through the axicons, done with Zemax; (c) Image of the beam profile at the objective lens inlet. Scale bar: 2.5mm; (d)-(e) Beam profiles at objective aperture, obtained by simulation. Scale bar: 2.5mm. The axicon A2 is positioned on axis in (d), and off axis by 0.5mm in both horizontal and vertical directions (e), showing a characteristic distortion pattern.

inlet position are similar. This trend confirms the results of [24], where the decay of trapping efficiency was shown as an increasing fraction of the Gaussian beam was blocked.

Figure 2 shows the setup used to obtain a hollow beam, and the beam profile from simulation results. The optical simulation in ZEMAX confirmed the inlet annular beam profile obtained using two conical lenses. The experimentally obtained beam profile before the objective lens is shown in Fig. 2(b). This beam was chosen to have the right radius to result in a high enough incidence angle and an evanescent field after the high NA objective lens. The beam intensity propagated beyond the sample for this case of hollow beam is similar to the two cases considered above (Gaussian and focused beams) in the off-axis TIR region. The trapping stiffness obtained with the hollow beam is also similar to that achieved with the Gaussian beam off axis, in the TIR region. The hollow beam trapping stiffness can be modulated and is reduced by moving the sample cell vertically (z axis): the $3\ \mu\text{m}$ diameter silica beads can be trapped up to around $10\ \mu\text{m}$ above the surface, $1.85\ \mu\text{m}$ diameter silica beads up to $4\ \mu\text{m}$ as shown in Fig. 3(c). Trapping near the surface was possible with 3 and $1.85\ \mu\text{m}$ diameter silica beads, but not possible with 1.0 and $0.5\ \mu\text{m}$ diameter silica and $2.0\ \mu\text{m}$ diameter polystyrene beads. These experimental results seem to imply that there is a weak potential capable of three dimensionally trapping beads, even away from the bottom surface. This could be caused by a fraction of the beam propagating vertically. The difference observed with particles of different density (silica and polystyrene) points to the fact that under these conditions stability needs to be achieved balancing all forces, including optical gradients and gravity.

Trapping of red blood cells with the focused evanescent field generated by the hollow beam

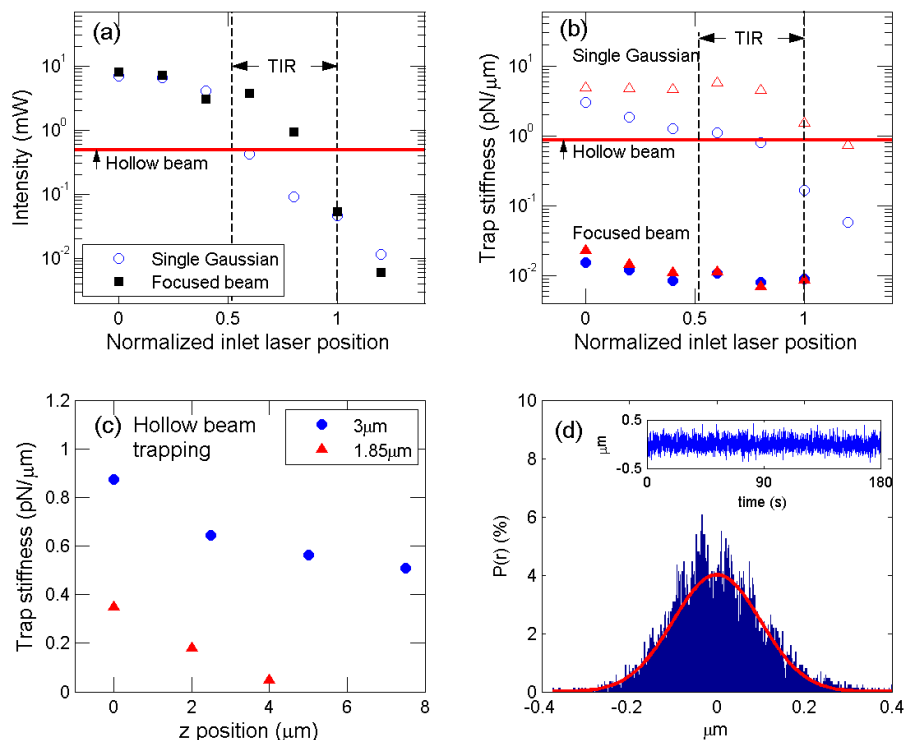


Fig. 3. Comparison between the optical setup geometries. (a) Laser intensity measurements after propagation through the objective and water-filled sample chambers. This is plotted as a function of the inlet laser position, normalized by the aperture radius. The region of TIR (total internal reflection) is highlighted by dotted lines. (b) The in-plane trap stiffness for $3\mu\text{m}$ diameter silica beads for the experiment with a Gaussian beam (\circ : stiffness in x direction, \triangle : stiffness in y direction) and for the focused beam experiment (\bullet : stiffness in x direction, \blacktriangle : stiffness in y direction). The trap stiffness obtained with the hollow beam is shown as a constant value for comparison. (c) Trap stiffness with the hollow beam, trapping $3\mu\text{m}$ and $1.85\mu\text{m}$ diameter silica beads, as a function of the height z at which the beads are trapped above the bottom surface. (d) Distribution of displacements from center of trap, for the $3\mu\text{m}$ diameter beads in a hollow beam trap at $z = 0$. The fit to a Gaussian (solid line) corresponds to eq. 1 and allows the trap stiffness to be determined. The inset shows the “raw data” of displacement as function of time.

is shown in Fig. 4(a). Cells, flowing in a square capillary, can be attracted to the bottom surface and maintained horizontal. After switching off the laser, the trapped cell is observed to flow. By comparison, the conventional geometry of Gaussian on axis beam (propagating field) leads to trapping the cell in a vertical configuration as shown in Fig. 4(b).

4. Discussion

We have measured that in the evanescent field conditions the trapping stiffness with a beam weakly focused on the back focal plane was three decades weaker than for the Gaussian beam. This result implies that to have significant trapping, a ring beam for the evanescent field trapping should propagate as parallel as possible to the optical axis. If the laser beam is focused before or inside objective lens, the trapping stiffness is made weaker although the trapping area is

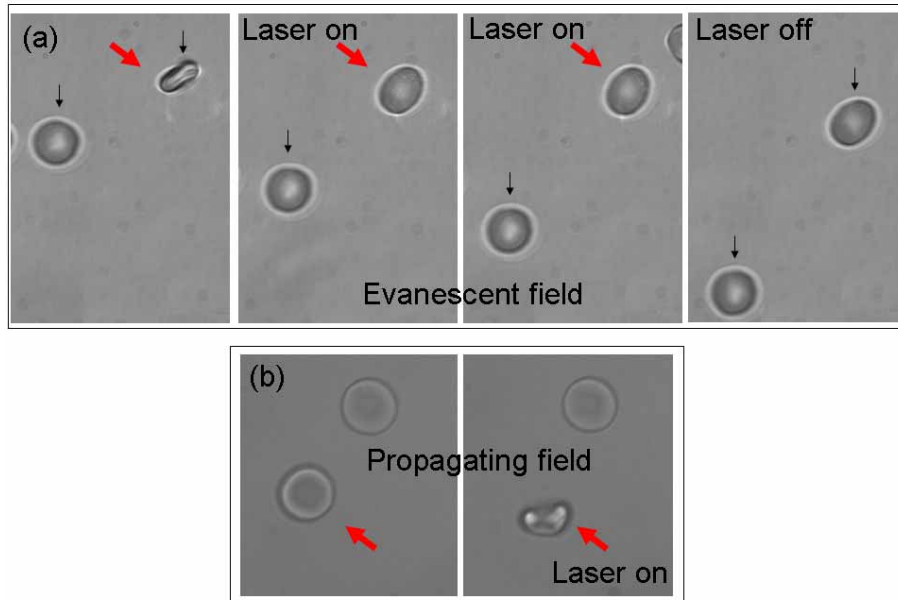


Fig. 4. Time sequence images of RBC that are trapped against flow with $v \simeq 0.66 \mu\text{m/s}$. The thick arrow indicates the cells that are trapped when the laser is on. The small arrows identify flowing cells. In (a) trapping is due to the evanescent field, and the RBC lies flat in the horizontal plane; In (b) the setup is with the standard on-axis Gaussian beam, propagating vertically. The RBC is trapped in the vertical plane.

correspondingly wider. The use of the telescopic pair of axicon lenses to generate the parallel ring beam seems optimal to achieve the right conditions for evanescent field trapping. Other attempts were made exploring the use of a single axicon and three convex lenses to make a focused ring beam before or inside the objective lens for the evanescent field, but in this configuration it was not possible to trap the micro-particles stably. This geometry leads to a broad spot on the interface plane and hence weak trapping. What is a disadvantage in trapping is however an advantage in TIR fluorescence imaging, where it is useful to have a large excitation area [29].

In this paper we show that using two axicon lenses is a simple and efficient way to make a parallel annular beam with the right characteristics to make an evanescent field for trapping. Comparing to the previous studies of Gu et al. [25, 26] where the central region of the objective inlet aperture was blocked by an opaque disk in order to provide the ring beam for the evanescent field, our optical setup with the conical lenses makes a more efficient use of the laser power.

As a preliminary application of the evanescent field trapping, we performed RBC manipulation under gravity-induced flow. The red blood cells have been shown to acquire a flat configuration on the surface towards which they are trapped. This may be beneficial in the future for investigations aiming to measure membrane activity and membrane bound proteins. The trapped cells are released back into the flow after the laser is turned off. An important advantage of using an evanescent field for trapping biological samples is to minimize the light that propagates through the sample, reducing the risk of photo-induced damage. This type of trap-

ping can be easily combined with TIR fluorescence imaging and should prove useful for future investigations on membrane activity and membrane bound proteins.

5. Conclusion

We have demonstrated the direct optical trapping of particles and cells with a focused evanescent field, generated by a ring beam obtained using two conical lenses and a high NA objective. We compared the new beam geometry with various other conditions of Gaussian and focused beams, entering the microscope objective on and off-axis. Finally, we applied the focused evanescent field to prove that erythrocytes can be manipulated under flow, and showed that the new optical beam geometry leads the cell to be trapped flat on the glass surface, an ideal conformation to observe the cell membrane. The use of focused evanescent field trapping obtained by conical lenses will facilitate new experiments requiring optical manipulation of biological cells taking advantage of the particular trapping field and laser efficiency.

Acknowledgments

We would like to thank Moritz Kreysing and Jochen Guck for useful suggestions and discussions. This work was supported by the Korea Foundation for International Cooperation of Science & Technology (KICOS) through a grant provided by the Korean Ministry of Education Science & Technology (MEST) in 2009-00591.